Original Article

Development and validation of a graph convolutional network (GCN)-based automatic superimposition method for maxillary digital dental models (MDMs)

Yichen Pan[a]; Zhechen Zhang[b]; Tianmin Xu[c]; Gui Chen[d]

ABSTRACT

Objectives: To validate the accuracy and reliability of a graph convolutional network (GCN)-based superimposition method of a maxillary digital dental model (MDM) by comparing it with manual superimposition and quantifying the clinical error from this method.

Materials and Methods: Based on a GCN, learning the features from 100 three-dimensional digital occlusal models under supervision of the palatal stable structure labels that were manually annotated by senior specialists, the palatal stable structure was automatically segmented. The average Hausdorff distance was calculated to assess the difference between automatic and manual segmentations. Tooth position and angulation, including rotation, tip, and torque, of bilateral upper first molars and central incisors were obtained to measure the clinical error of automatic superimposition. Reliability was calculated by intraclass correlation coefficient (ICC).

Results: The average Hausdorff distance was 0.36 mm between automatic and manual segmentations of the palatal stable region and was larger than the intraexaminer and interexaminer deviations. The tooth position deviation was <0.32 mm, and the tooth angulation difference was $<0.26°$ for tip and torque, and 0.46–0.61° in rotation. ICCs, used for assessment of reliability, ranged from 0.82 to 0.99 in all variables.

Conclusions: The GCN-based MDM superimposition is an efficient method for the assessment of tooth movement in adults. The clinical error in tooth position and angulation induced by the method was clinically acceptable. Reliability was as high as manual segmentation. (*Angle Orthod*. 2025;95:259–265.)

KEY WORDS: Digital dental model; Graph convolutional network; Superimposition; Accuracy and reliability; Palatal stable region

[a] Postdoctoral Researcher, Department of Oral and Maxillofacial-Head Neck Oncology, College of Stomatology, Shanghai Ninth People's Hospital, Shanghai Jiao Tong University School of Medicine, Shanghai, People's Republic of China.

[b] Associate Professor, Department of Orthodontics, College of Stomatology, Shanghai Ninth People's Hospital, Shanghai Jiao Tong University School of Medicine, Shanghai, People's Republic of China.

[c] Professor, Department of Orthodontics, Peking University School and Hospital of Stomatology, Beijing, People's Republic of China.

[d] Associate Professor, Department of Orthodontics, Peking University School and Hospital of Stomatology, Beijing, People's Republic of China.

Corresponding author: Dr Gui Chen, Associate Professor, Department of Orthodontics, Peking University School and Hospital of Stomatology, No. 22 Zhongguancun S Ave, Haidian District, Beijing 100081, People's Republic of China (e-mail: chengui723@163.com)

Accepted: December 22, 2024. Submitted: July 12, 2024.
Published Online: February 18, 2025

INTRODUCTION

Typical orthodontic treatment requires obtaining various information from patients. A dental model is an irreplaceable tool that accurately and clearly duplicates tooth position, tooth shape, and occlusal relationships. The popularization of oral scanning improved the use of digital dental models in clinical practice. Without x-ray exposure, digital dental models can be obtained repeatedly during treatment to record progression of tooth movement.

Measurement of tooth movement is especially important in orthodontic outcome evaluation. Historically, measurement of orthodontic tooth movement and bone growth have been based on superimposition on the stable areas that change only minimally during treatment.[1] Analysis of treatment and growth changes in tooth and bone can be traced back to Björk et al.,[2–4] who adopted a cephalometric superimposition method based on metallic implants. Ruan et al.[5] used metallic

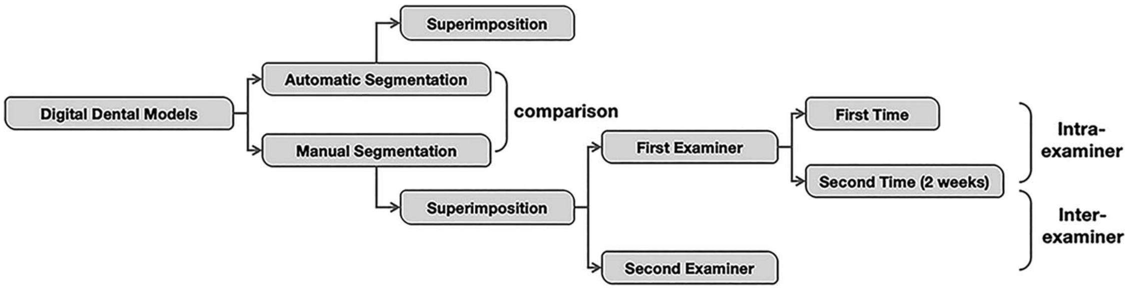

Figure 1. Flowchart of the study procedure.

implants as stable anchors in cone beam computed tomography (CBCT) images to evaluate tooth movement. For digital dental models, Chen et al.[6] proposed a maxillary digital dental model (MDM) superimposition method based on the stable region including the medial 2/3 of the third palatal rugae and the adjacent palatal vault region. This MDM superimposition was already validated in a previous study[7] to be as accurate and reliable as CBCT voxel-based superimposition in adult patients.

Usually, the processing of digital dental models transfers STL files into point clouds, or they are imported as mesh surfaces.[8,9] At present, application of an artificial intelligence–assisted approach to analyze a digital dental model is most commonly used for tooth crown segmentation.[10,11] Graph convolutional networks (GCNs) have been widely used in analysis of three-dimensional (3D) medical imaging.[12–15] In the current study, we creatively propose a GCN-based superimposition method for digital dental models. The study was designed to validate the accuracy of this method by comparing automatic segmentation with manual segmentation and quantifying the clinical error in measuring tooth movement by MDM superimposition between an automatically and manually segmented palatal stable region.

MATERIALS AND METHODS

Patients and Dental Casts

Dental casts were collected from consecutive patients from the Department of Orthodontics, Peking University School and Hospital of Stomatology. Exclusion criteria were patients under 18 years old, patients with craniofacial abnormalities, craniofacial surgery or trauma history, and dental casts of low quality. The dental casts collected were scanned by an R700 linear laser scanner (3Shape Corp., Copenhagen, Denmark) and saved in stereolithography interface (STL) format. The procedure of this study is illustrated in Figure 1. Informed consent was signed by all the patients, and the research protocol was approved by the Institutional Review Board of Peking University School and Hospital of Stomatology (IRB00001052-09010).

Training for the Automatic Stable Region Segmentation

The reference area for superimposition was defined as the medial 2/3 of the third rugae and the adjacent regional palatal vault in front of the most distal points of upper first molars.[6] Authors of a previous study showed that this method was as accurate and repeatable as CBCT voxel-based superimposition in adults.[7] Labeling of the stable regions of 100 MDMs was conducted using MeshLab (version 2022, Visual Computing Lab of ISTI-CNR, Pisa, Italy), and all labels were checked by two senior specialists (Figure 2), from which 80 were used as training samples and 20 as test samples.

This network extracted the features of each vertex on the MDM under the supervision of the labels manually annotated by specialists and trained a binary vertex classifier to predict the probability that each vertex of the model belonged to the palatal stable region. The network adopted a supervised training method and

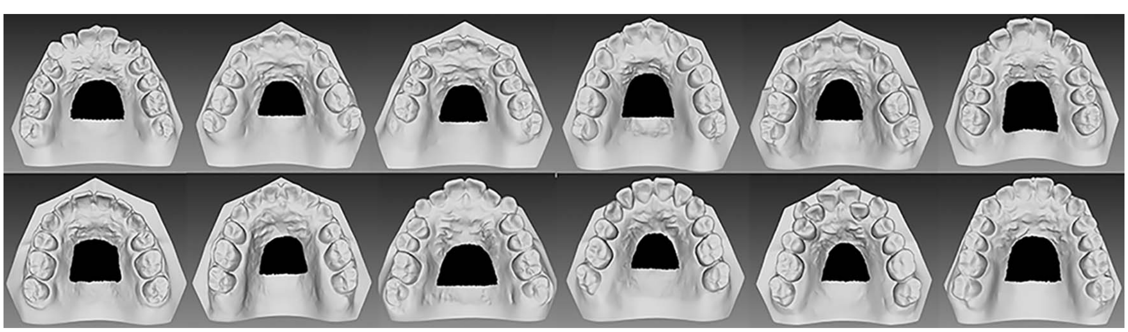

Figure 2. Labeling of the palatal stable region in Meshlab2022.

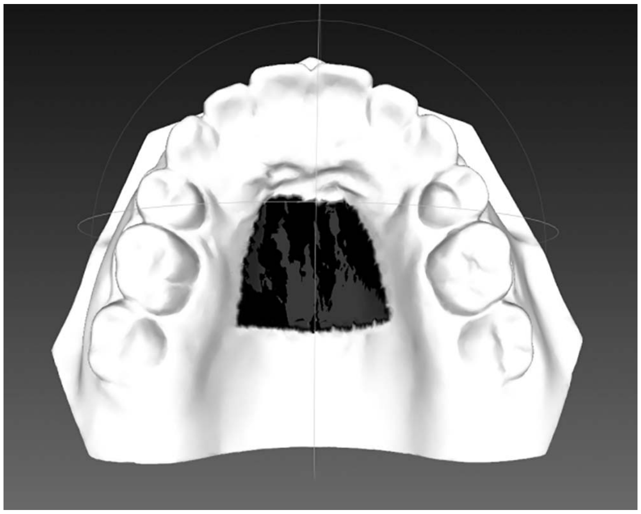

Figure 3. Superimposition of automatic segmentation (gray) and manual labeling (black).

used a loss function, which was to be minimized, to calculate the difference between the manually annotated labels (ground truth) and the network estimated labels of the MDM to optimize the network parameters.

Testing of the Automatic Segmentation Network

Testing of the network was done by making comparisons between automatic and manual segmentations. For the newly input MDM, the vertex features and their adjacency relationships extracted from the MDM were input into the trained network, which could output the probability prediction of the palatal stable region for each vertex. The automatic segmentation could be completed by binary classification based on a predefined threshold. The set of vertices predicted as palatal stable regions constituted the segmentation result.

In MeshLab2022, the automatic and manual segmentations were extracted as two single layers (Figure 3). The average Hausdorff distance (Table 1) could be calculated automatically in a built-in function in MeshLab2022 to measure the difference between the two segmented layers. Two examiners repeated all the measurements after 2 weeks.

Accuracy of Automatic Superimposition

The pretreatment and posttreatment models were imported into Rapidform2006 (INUS Technology Inc., Seoul, Korea). Two posttreatment models were superimposed by automatically and manually segmented stable regions denoted as AS (automatic superimposition) and MS (manual superimposition), respectively. Position and angulation of bilateral upper first molars and central incisors were measured to appraise the clinical error.

A coordinate system was created on the pretreatment model. The functional occlusal plane (FOP) was defined as the transverse plane (Table 1). Then two points on the palatal suture were marked as A and B (Figure 4a) and projected on the transverse plane as A′ and B′ (Figure 4b). The A, B and A′, B′ points were used to compose the midsagittal plane (Figure 4a). The B′ point was set as the origin of the coordinate system, B′A′ as the *x* axis, and B′B as the *y* axis (Figure 4c).

Measurement of tooth position and angulation were elaborated in a previous study[7] (Table1, Figure 4d–h). Tooth position was represented by the values of coordinates (*x*, *y*, *z*) of the U6 mesial-buccal cusp (Figure 4d) and the midpoint of the U1 incisal edge (Figure 4e). Tooth angulation was represented by the angle between reference planes and tooth axes (Table 1, Figure 4f–h). To eliminate the method error caused by the identification of crown landmarks, the dental crowns together with crown landmarks were transferred from the MS model to the AS model in Rapidform2006 (Figure 4i–k).

Table 1. Definitions of the Variables and Other Concepts Used in this Study

Items	Definition
Hausdorff mean	The average of all the distances from a point in one surface to the closest point in the other surface
Hausdorff RMS	The root mean square (RMS) of all the distances from a point in one surface to the closest point in the other surface
RU1 (LU1, RU6, LU6)	Right upper central incisor (left upper central incisor, right upper first molar, and left upper first molar)
x (*y*, *z*)	Value of coordinate along the *x* (*y*, *z*) axis in the three-dimensional coordinate system constructed on the pretreatment model
Functional occlusal plane (FOP)	The transverse plane calculated by the fitted plane of both cusps of bilateral maxillary first premolars, second premolars, and first molars
Midsaggital plane	Composed of two points marked on the palatal suture and their projected points on the FOP
U6 tooth axis	Connection of the most occlusal and gingival points (D and E) of the buccal groove (Figure 4d)
U1 tooth axis	Connection of the midpoint of the incisal edge and the gingival edge (F and I; Figure 4e)
Mesiodistal plane	Formed by the distal and mesial points along the occlusal central groove (U6) or the incisal edge (U1) and their projected points on the FOP
Buccolingual plane	Generated by the plane perpendicular to both the mesiodistal plane and FOP passing through either distal or mesial point
Rotation	The angle between the mesiodistal plane and the midsagittal plane (Figure 4f)
Tip	The angle between the projection of tooth axis on buccolingual plane and the normal direction of the FOP (Figure 4g)
Torque	The angle between the projection of tooth axis on the mesiodistal plane and the normal direction of the FOP (Figure 4h)

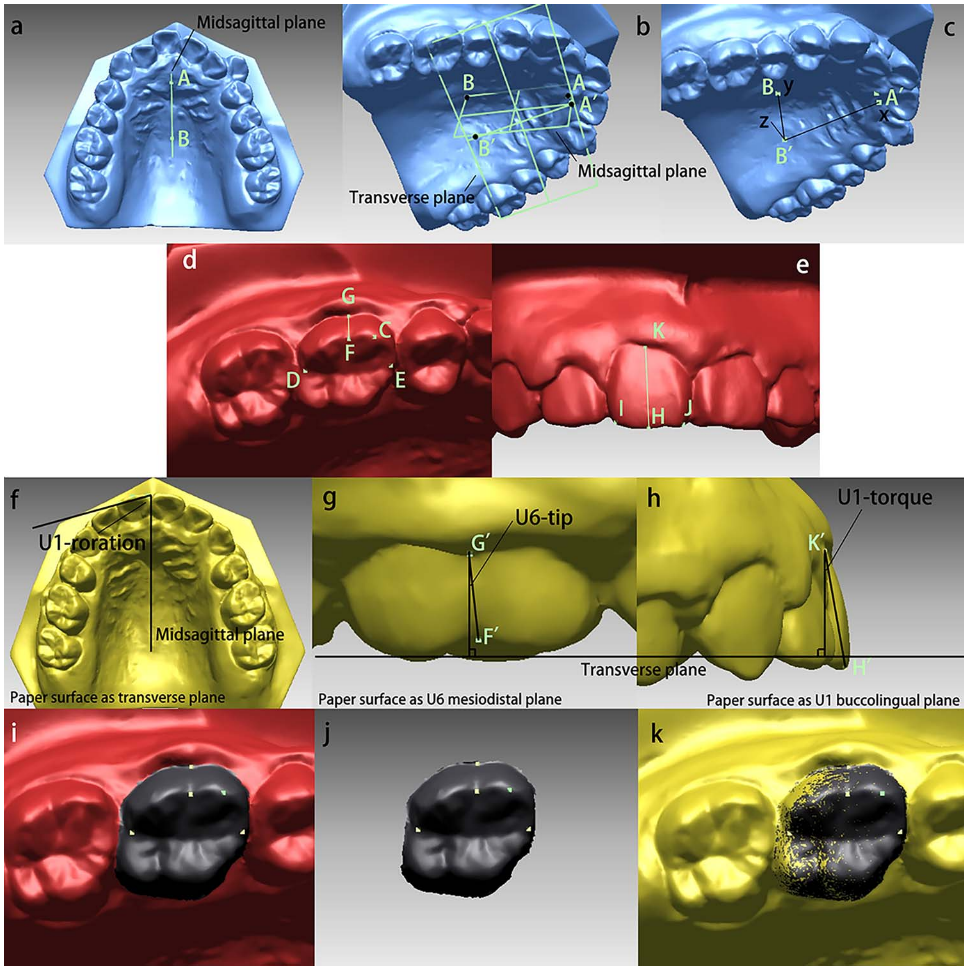

Figure 4. (a) Palatal suture landmarks (A, front point of palatal suture; B, back point of palatal suture). (b) Midsagittal plane and transverse plane (A′, B′, projected points of A, B on the transverse plane). (c) Coordinate system on the pretreatment model. (d) Landmarks of U6s (C, mesial-buccal cusp; D, most distal point; E, most mesial point; F, occlusal point of buccal groove; and G, gingival point of buccal groove). (e) Landmarks of U1s (H, midpoint of incisal edge; I, most distal point of incisal edge; J, most mesial point of incisal edge; and K, midpoint of gingival edge). (f) Measurement of U1 rotation. (g) Measurement of U6 tip. (h) Measurement of U1 torque. (i)–(k) Landmark transference by (j) tooth crown area from (i) manual superimposition (MS) model to (k) automatic superimposition (AS) model.

Statistical Analysis

Sample size calculation was conducted in Power Analysis and Sample Size (PASS) version 15.0.1 software (NCSS LLC, East Kaysville, UT). To achieve a power <0.80 with the largest true mean as 0.6 and a standard deviation of 1.5, sample size was calculated to be <9.

In SPSS Statistics version 23.0 (IBM, Armonk, NY), one-sample *t*-tests were conducted by comparing the 3D deviations of AS and MS models with zero to evaluate the accuracy of AS of MDM, based on automatic identification of the stable region of the palatal vault. An error of <1 mm was considered clinically acceptable.[16,17] The intraclass correlation coefficient (ICC) was used to assess the reliability of superimposition. A *P* value of $<.05$ was considered statistically significant.

RESULTS

Accuracy and Reliability of Stable Region Segmentation

The average absolute distance from the border of automatic to manual segmentation was 0.36 mm (Table 2).

Table 2. Hausdorff Distance (mm) of the Manual Superimposition (MS) and Automatic Superimposition (AS)[a]

Comparisons	Variables	Mean, mm (95% CI)
MS vs AS	Hausdorff mean	0.36 (0.15, 0.58)
	Hausdorff RMS	0.60 (0.29, 0.92)
Intraexaminer	Hausdorff mean	0.07 (0.04, 0.11)
	Hausdorff RMS	0.27 (0.17, 0.37)
Interexaminer	Hausdorff mean	0.06 (0.03, 0.10)
	Hausdorff RMS	0.25 (0.16, 0.34)

[a] CI indicates confidence interval; RMS, root mean square.

Table 3. Deviation of Tooth Position and Tooth Angulation Between Automatic Superimposition (AS) and Manual Superimposition (MS) Models[a]

Variable	Mean (95% CI)	*P*
RU6-*x*	0.32 (−0.13, 0.76)	.139
RU6-*y*	−0.04 (−0.23, 0.16)	.699
RU6-*z*	−0.09 (−0.22, 0.04)	.151
LU6-*x*	−0.1 (−0.55, 0.34)	.610
LU6-*y*	0.09 (−0.3, 0.48)	.618
LU6-*z*	−0.09 (−0.22, 0.03)	.128
RU1-*x*	0.14 (−0.01, 0.29)	.060
RU1-*y*	−0.06 (−0.44, 0.33)	.752
RU1-*z*	−0.3 (−0.78, 0.18)	.191
LU1-*x*	0.08 (−0.07, 0.23)	.282
LU1-*y*	−0.03 (−0.5, 0.44)	.882
LU1-*z*	−0.3 (−0.78, 0.18)	.193
RU6-rotation	0.48 (−0.42, 1.38)	.256
RU6-tip	0.26 (−1.05, 0.53)	.475
RU6-torque	−0.08 (−0.71, 0.56)	.794
LU6-rotation	−0.61 (−1.54, 0.31)	.168
LU6-tip	0.08 (−0.43, 0.59)	.718
LU6-torque	0.05 (−0.85, 0.95)	.898
RU1-rotation	0.52 (−0.4, 1.43)	.235
RU1-tip	−0.14 (−0.82, 0.55)	.666
RU1-torque	−0.18 (−0.79, 0.44)	.529
LU1-rotation	−0.46 (−1.36, 0.45)	.282
LU1-tip	0.07 (−0.22, 0.37)	.587
LU1-torque	−0.11 (−0.9, 0.68)	.759

[a] CI indicates confidence interval. Significance level was set at $P < .05$.

The difference between automatic and manual segmentations was a bit larger than the intraexaminer and interexaminer average differences, which were both <0.10 mm. The root mean square (RMS), which is naturally larger than the arithmetic mean in mathematics, was 0.60 mm in this study. The image of segmented models was specifically analyzed, and it was found that the largest deviation was usually seen in the posterior border of the stable region.

Accuracy of AS

The difference in tooth position and angulation could represent the clinical error derived from the AS method. For all variables, no significant difference was found between the superimpositions based on automatic and manual palatal region segmentations (Table 3). Clinically, the average deviation ranged from 0.03 mm to 0.32 mm in tooth position, and 0.01° to 0.61° in tooth angulation. Specifically, the average difference in tooth tip and torque between the AS and MS was 0.01–0.26°, and the largest deviation was observed in tooth rotation ranging from 0.46° to 0.61°.

Reliability of AS

Reliability was calculated by ICC. An ICC >0.75 was considered acceptable reliability. Both intraexaminer and interexaminer ICCs ranged from 0.87 to 0.99 for tooth position and 0.82 to 0.99 for tooth angulation. The intraexaminer ICC was between 0.92 and 0.99, and the interexaminer ICC was slightly lower. The overall consistency between MS and AS ranged from 0.87 to 0.99. The least consistency was observed in the *y* direction of the coordinate axis, ranging from 0.87 to 0.96, and in tooth rotation, ranging from 0.82 to 0.97.

DISCUSSION

In this study, we proposed a new, automatic MDM superimposition method based on GCN and validated the accuracy and reliability of the method compared with MS. It was found that the newly proposed method was almost as accurate and reliable as MS and can be of great help in clinical practice.

Deep learning–assisted segmentation in dental models have been widely used for the tooth crown area.[18] Compared with crown areas, the surface of the palatal region is not as rugged and lacks characteristic structures like dental cusps and grooves, making it harder for segmentation training tasks.[19,20]

The Hausdorff distance indicates the largest distance from a point in one set to the closest point in the other set, being vulnerable to outliers, and is used to assess border differences between two images.[21,22] In this study, the average Hausdorff distance was used to diminish the influence of outliers.[23] The average Hausdorff distance was 0.36 mm in this study, which is not a substantial value clinically. The largest deviation was found in the posterior border of the segmented area. The clinical definition of the posterior border was the most distal point of the bilateral first molars,[6] but in some patients, the left and right first molars were not strictly symmetric, which might have confused the training model. The mean Hausdorff distance in automatic segmentation was a bit larger than in manual segmentation by about 0.3 mm, but both were clinically acceptable.

Generally, iterative closest point superimposition has been applied to align two selected surfaces.[24,25] In several commercial software applications, local surface superimposition can be done after a gross alignment based on reference points.[26–28] This process usually takes 3 to 5 minutes for skilled operators. The superimposition of multiple stage models may take >10 minutes for models from only one patient. AS would save a great amount of time for researchers.[29]

Authors of a previous study showed that MDM superimposition was as accurate and reliable as CBCT superimposition.[7] Generally, 1 mm has been considered to be clinically acceptable in cephalometric analysis.[16,17] Moon et al.[30] developed a computer-aided cephalometric superimposition, but the error was >1 mm. Additionally, Moon et al.[31] developed a deep learning–based approach to superimpose soft tissue landmarks on digital photographs and lateral cephalometric radiographs, and the positional difference with the manual approach was generally around 0.1 mm to 0.5 mm. Xiao et al.[32] used 3D facial scanning features as the basis for MDM superimposition and achieved a clinical error of <0.42 mm and 0.92°. In the current study, the average deviation in tooth position was <0.32 mm, which is clinically acceptable and no larger than the deviation between MDM and CBCT superimposition in a previous study.[7] In this study, the average deviation in tooth angulation was $<0.26°$ in tooth tip and torque and ranged from 0.46° to 0.61° in rotation. Compared with a previous study, the clinical error was basically equal in tooth tip and torque.[7] Tooth rotation was not measured in the previous study,[7] but in this study, the greatest difference between AS and MS was detected in tooth rotation. This phenomenon may be explained by the shape of the palatal region. Tooth rotation was defined as the angle between the midsagittal plane and the tooth mesiodistal plane which is an angle parallel to the transverse plane. The palatal vault, approximately a smooth curved surface, also lies transversely and is, therefore, less resistant to positional changes in the transverse orientation. Therefore, it is suggested that a smoothing procedure not be conducted because smoothing may reduce roughness of the palatal surface and decrease the identifiability of palatal structures.[33]

Although segmentation of the stable region was not exactly as accurate as defined, superimposition based on this region still showed high accuracy and reliability. The identification of palatal stable regions themselves was a bit subjective, although the border was defined, but in clinical use, the superimposition was based on the inner shape of the 3D palatal surface rather than the edge. Additionally, the difference was only a bit larger than MS, showing promise for clinical use.

CONCLUSIONS

- The GCN-based automatic MDM superimposition is an efficient method for the assessment of tooth movement in adults.
- The clinical error induced by AS was clinically acceptable.
- Reliability of the method is as high as manual segmentation and sufficient for clinical practice.

ACKNOWLEDGMENTS

This work was supported by Beijing Natural Science Foundation (Grant L242134). We would like to thank Diya Sun and Prof. Yuru Pei from Key Laboratory of Machine Perception, Department of Machine Intelligence, Peking University, for technical support in model training.

REFERENCES

1. Gu Y, McNamara JA Jr. Cephalometric superimpositions. *Angle Orthod.* 2008;78(6):967–976.
2. Björk A. Variations in the growth pattern of the human mandible: longitudinal radiographic study by the implant method. *J Dent Res.* 1963;42(1)Pt 2:400–411.
3. Björk A. Facial growth in man, studied with the aid of metallic implants. *Acta Odontol Scand.* 1955;13(1):9–34.
4. Björk A, Skieller V. Growth of the maxilla in three dimensions as revealed radiographically by the implant method. *Br J Orthod.* 1977;4(2):53–64.
5. Ruan MJ, Chen G, Xu TM. Comparison of orthodontic tooth movement between adolescents and adults based on implant superimposition. *PLoS One.* 2018;13(5):e0197281.
6. Chen G, Chen S, Zhang XY, et al. Stable region for maxillary dental cast superimposition in adults, studied with the aid of stable miniscrews. *Orthod Craniofac Res.* 2011;14(2):70–79.
7. Pan Y, Wang X, Dai F, Chen G, Xu T. Accuracy and reliability of maxillary digital model (MDM) superimposition in evaluating teeth movement in adults compared with CBCT maxillary superimposition. *Sci Rep.* 2020;10(1):19384.
8. Zhao Y, Zhang L, Liu Y, et al. Two-stream graph convolutional network for intra-oral scanner image segmentation. *IEEE Trans Med Imaging.* 2022;41(4):826–835.
9. Xu X, Liu C, Zheng Y. 3D Tooth segmentation and labeling using deep convolutional neural networks. *IEEE Trans Vis Comput Graph.* 2019;25(7):2336–2348.
10. Im J, Kim JY, Yu HS, et al. Accuracy and efficiency of automatic tooth segmentation in digital dental models using deep learning. *Sci Rep.* 2022;12(1):9429.
11. Li J, Cheng B, Niu N, et al. A fine-grained orthodontics segmentation model for 3D intraoral scan data. *Comput Biol Med.* 2024;168:107821.
12. Liu M, Li X, Liu J, Liu W, Yu Z. TUCNet: a channel and spatial attention-based graph convolutional network for teeth upsampling and completion. *Comput Biol Med.* 2023;166:107519.
13. Mao C, Yao L, Luo Y. ImageGCN: multi-relational image graph convolutional networks for disease identification with chest x-rays. *IEEE Trans Med Imaging.* 2022;41(8):1990–2003.
14. Ma T, Zhou X, Yang J, et al. Dental lesion segmentation using an improved ICNet network with attention. *Micromachines.* 2022;13(11):1920.
15. Song TA, Roy Chowdhury S, Yang F, et al. Graph convolutional neural networks for Alzheimer's disease classification. *Proc IEEE Int Symp Biomed Imaging.* 2019;2019:414–417.
16. Ghafari J, Engel FE, Laster LL. Cephalometric superimposition on the cranial base: a review and a comparison of four methods. *Am J Orthod Dentofacial Orthop*. 1987;91:403–413.
17. Huja S, Grubaugh E, Rummel A, Fields H, Beck F. Comparison of hand-traced and computer-based cephalometric superimpositions. *Angle Orthod*. 2009;79:428–435.
18. Cui Z, Li C, Chen N, et al. TSegNet: an efficient and accurate tooth segmentation network on 3D dental model. *Med Image Anal.* 2021;69:101949.
19. Osman R, Alharbi N. Does the palatal vault form have an influence on the scan time and accuracy of intraoral scans of completely edentulous arches? An in-vitro study. *J Adv Prosthodont.* 2022;14(5):294–304.
20. Hamed HAE, Hebeshi AM, Husseiny E. Effect of palatal vault depth on the trueness of metal laser-sintered and cast cobalt-

chromium removable partial denture frameworks. *J Prosthodont.* 2023;32(4):353–360.
21. Lange K. Computation of the Hausdorff distance between two compact convex sets. *Algorithms.* 2023;16(10):471.
22. Karimi D, Salcudean SE. Reducing the Hausdorff distance in medical image segmentation with convolutional neural networks. *IEEE Trans Med Imaging.* 2020;39(2):499–513.
23. Aydin OU, Taha AA, Hilbert A, et al. On the usage of average Hausdorff distance for segmentation performance assessment: hidden error when used for ranking. *Eur Radiol Exp.* 2021;5(1):4.
24. Choi O, Park MG, Hwang Y. Iterative *K*-closest point algorithms for colored point cloud registration. *Sensors* 2020;20(18):5331.
25. Tsumura R, Morishima Y, Koseki Y, Yoshinaka K. Body surface registration considering individual differences with non-rigid iterative closest point. *Int J Comput Assist Radiol Surg.* 2023;18(8):1511–1520.
26. Bazina M, Cevidanes L, Ruellas A, et al. Precision and reliability of Dolphin 3-dimensional voxel-based superimposition. *Am J Orthod Dentofacial Orthop.* 2018;153(4):599–606.
27. Dindaroğlu F, Duran GS, Aras I. Three-dimensional evaluation of morphologic tooth symmetry in various malocclusions. *Am J Orthod Dentofacial Orthop.* 2016;150(3):459–466.
28. Nichols DA, Gardner G, Carballeyra AD. Reproducibility of bracket positioning in the indirect bonding technique. *Am J Orthod Dentofacial Orthop.* 2013;144(5):770–776.
29. Vaassen F, Hazelaar C, Vaniqui A, et al. Evaluation of measures for assessing time-saving of automatic organ-at-risk segmentation in radiotherapy. *Phys Imaging Radiat Oncol.* 2020;13:1–6.
30. Moon JH, Hwang HW, Lee SJ. Evaluation of an automated superimposition method for computer-aided cephalometrics. *Angle Orthod*. 2020;90(3):390–396.
31. Moon JH, Kim MG, Cho SJ, et al. Evaluation of automated photograph-cephalogram image integration using artificial intelligence models. *Angle Orthod*. 2024;94(6):595–601.
32. Xiao Z, Liu Z, Gu Y. Integration of digital maxillary dental casts with 3D facial images in orthodontic patients. *Angle Orthod*. 2019;90:397–404.
33. Veneziano A, Landi F, Profico A. Surface smoothing, decimation, and their effects on 3D biological specimens. *Am J Phys Anthropol.* 2018;166(2):473–480.